



Original Research Breast Imaging

Correlation analysis of multiparametric magnetic resonance imaging features and molecular subtypes of breast cancer

Junping Li¹, Guanghui Huo², Xiaoye Lei³, Guang Li¹, Mengxing Yu⁴, Ziyang Nie⁵, Zhenhua Guo¹, Yue Zhang¹

¹Department of Radiology, Xiangyang No.1 People's Hospital, Hubei University of Medicine, Xiangyang, Hubei, ²Department of Radiology, Mesclor Medical Imaging Diagnostic Center, Tianjin, Departments of ³Thyroid Gland Breast Surgery and ⁴Pathology, Xiangyang No.1 People's Hospital, Hubei University of Medicine, Xiangyang, Hubei, ⁵School of Life Sciences, Central China Normal University, Hubei Province, Wuhan, China.



***Corresponding author:**

Yue Zhang,
Department of Radiology,
Xiangyang No.1 People's
Hospital, Hubei University of
Medicine, Xiangyang, Hubei,
China.

80025846@qq.com

Received: 26 November 2024

Accepted: 25 May 2025

Published: 04 October 2025

DOI

10.25259/JCIS_162_2024

Quick Response Code:



ABSTRACT

Objectives: This study aims to evaluate the relationship between multiparametric magnetic resonance imaging (MRI) features – including T2-weighted imaging (T2WI), apparent diffusion coefficient (ADC), and dynamic contrast enhancement (DCE) – and molecular subtypes of breast cancer, to enhance non-invasive diagnostic stratification.

Material and Methods: This retrospective study enrolled 134 consecutive patients with pathologically confirmed breast cancer. A comparative analysis was performed to evaluate intergroup variations in clinicopathological characteristics, morphological features, and multiparametric MRI parameters (including T2WI signal intensity, ADC value, early-phase enhancement rate, and time-intensity curve pattern) across the four molecular subtypes.

Results: The cohort comprised 134 breast cancer patients stratified into molecular subtypes as follows: Luminal A ($n = 22, 16.4\%$), Luminal B ($n = 82, 61.2\%$), human epidermal growth factor receptor-2 (HER-2) (+) ($n = 13, 9.7\%$), and triple-negative breast cancer (TNBC) ($n = 17, 12.7\%$). Among the subtypes, there were statistically significant differences in terms of age, Ki-67 index, mass shape, margin, internal enhancement characteristic, T2WI signal, ADC value, early enhancement rate, and time intensity curve (TIC) pattern ($P = 0.025$; $P < 0.001$; $P = 0.039$; $P < 0.001$; $P = 0.043$; $P = 0.014$; $P < 0.001$; $P = 0.009$; and $P = 0.020$, respectively). Luminal subtypes predominantly exhibited irregular shapes, unclear/spiculated margins, heterogeneous enhancement, and uneven hypointense or isointense signal on T2WI. TNBC displayed regular shapes with smooth margins, ring enhancement, and uneven high signal on T2WI. The mean ADC value was significantly higher in HER-2 (+). Luminal A exhibited the highest early enhancement rate, while HER-2 (+) demonstrated the lowest. Analysis of TIC pattern revealed that type III curves were predominant across all subtypes, with a higher proportion observed in Luminal A and TNBC compared to Luminal B and HER-2 (+). Notably, no significant differences were observed between molecular subtypes in terms of menopausal status, axillary node metastasis, lesion type, number, size, and distribution, internal characteristics of non-mass enhancement lesions ($P > 0.05$).

Conclusion: Multiparametric MRI features, particularly ADC values, DCE kinetics, and T2WI signals, demonstrate significant associations with breast cancer molecular subtypes. These imaging biomarkers offer potential for non-invasive subtype prediction, supporting more tailored diagnostic and treatment strategies.

Keywords: Breast cancer, Immunohistochemistry, Molecular subtypes, Multiparametric magnetic resonance imaging

INTRODUCTION

Breast cancer is the leading cause of cancer-related mortality among women worldwide and remains the most frequently diagnosed malignant tumor. Alarming, there has been a noticeable trend toward earlier ages of onset in recent years.^[1] Breast cancer is a heterogeneous disease characterized by diverse phenotypes, each requiring tailored therapeutic strategies and exhibiting distinct prognoses.^[2-4] According to the St. Gallen 2013 consensus,^[5] breast cancer is classified into four molecular subtypes: Luminal A, Luminal B, human epidermal growth factor receptor 2 (HER-2+) overexpression, and triple-negative breast cancer (TNBC).

Diverse molecular subtypes of breast cancer vary in disease mode, responses to treatment, prognosis, and survival rates. The Luminal A subtype is characterized by well-differentiated tumor cells and carries the most favorable prognosis, with the lowest rates of local recurrence and metastasis. The Luminal B tumors are less differentiated, exhibit lower levels of estrogen receptor (ER) and progesterone receptor (PR) expression, and are associated with a worse prognosis compared to Luminal A. Both luminal subtypes commonly metastasize to the bone and demonstrate sensitive to hormone therapy. HER-2 overexpression subtype typically has moderate to high nuclear grade and is most common associated with liver and brain metastases. This subtype is most effectively treated with HER-2-targeted therapies. TNBC, on the other hand, is distinguished by its aggressive nature, poor prognosis, high risk of early recurrence, and frequent distant organ metastasis, particularly to the lungs and brain. Chemotherapy is the main treatment for TNBC.^[6,7] While selective biopsy tissue samples have been evaluated for the histopathological characteristics of tumor tissues, this often represents only a portion of the heterogeneous tumor, and this limited sampling may not be sufficient to capture the tumor heterogeneity that impacts tumor progression and treatment processes.^[8]

Breast multiparametric magnetic resonance imaging (MRI) is the most accurate and sensitive diagnostic imaging technology for detecting breast cancer, widely used in breast cancer screening, differentiation between benign and malignant breast lesions, pre-operative staging of breast cancer, pre-operative or post-operative evaluation of breast-conserving surgery, and assessment after neoadjuvant chemotherapy. MRI has fine tissue resolution, allowing us to observe the morphological and functional characteristics of the entire tumor *in vivo* and predict tumor molecular subtypes through imaging examinations. This may provide prominent contributions to the development of early treatment plans and understanding of prognosis in clinical practice.^[3,9,10] Previous extensive research had investigated the role of T2-weighted imaging (T2WI) imaging features, the apparent diffusion coefficient (ADC), or dynamic

contrast enhancement (DCE) in predicting breast cancer molecular subtypes.^[10-14] Nevertheless, there is currently no definitive consensus on the MRI imaging features of the various molecular subtypes of breast cancer.

The aim of our study is to evaluate the relationship between breast multiparametric MRI features (T2WI, ADC value, and DCE) imaging features and different molecular subtypes of breast cancer. The significance of this study is to predict the non-invasive molecular subtypes of pre-operative breast cancer, so as to reduce unnecessary needle biopsy, and guide clinicians to choose the most appropriate treatment.

MATERIAL AND METHODS

Patient general information

A retrospective analysis of cases diagnosed with breast cancer in our hospital from April 2021 to May 2024 who underwent pre-operative breast MRI examinations. Inclusion criteria are as follows: (1) confirmed as breast cancer by pre-operative pathology; (2) no prior surgery, chemotherapy, radiotherapy, or other drug treatments before the MRI examination for all patients; and (3) complete information on ER, PR, HER-2, and Ki-67 status for determining molecular subtypes. Exclusion criteria are as follows: Poor MRI image quality rendering assessment impossible. This study has been approved by our Hospital's Ethics Committee, with the exemption of informed consent from participants (NO. XYYYYE20220091). This study was conducted in accordance with the tenets of the Declaration of Helsinki.

MRI protocol

All the patients were examined in the prone position on the 3.0T MRI system (Ingenia deoxyribonucleic acid; Philips medical system) with the accompanying intellispace portal (ISP), post-processing workstation using a 16-channel dedicated bilateral breast matrix coil. Scanning parameters and sequences included: (1) axial T2WI with fat suppression: Field of view (FOV) 320 mm × 320 mm, slice thickness 4 mm, interslice gap 0.4 mm, TR = 4000 ms, TE = 80 ms, flip angle 90°, excitation 1; (2) diffusion-weighted imaging (DWI) using an echo planar imaging (EPI) sequence: FOV 300 mm × 120 mm, slice thickness 4 mm, interslice gap 0.4 mm, repetition time (TR) = 3500 ~ 5000 ms, Echo Time (TE) = 88 ms, flip angle 90°, excitation 1, b-values of 0, 50, 100, 200, 500, 1000, 2000 s/mm²; and (3) DCE using the dyn_eTHRIVE sequence: FOV 250 mm × 340 mm, slice thickness 1 mm, TR = 4.5 ms, TE = 2 ms, excitation 1. The contrast agent (gadopentetic acid) was injected into a high-pressure syringe at the flow rate of 2.5 mL/s, 0.2 mmol/kg, followed by 15 ml of saline at the same flow rate. The pre-contrast scan was followed by six consecutive dynamic enhanced scans with a temporal resolution of 88 s per phase.

Image processing and analysis

Two radiologists with expertise in breast MRI diagnosis – one chief physician and one attending physician – independently evaluated breast lesions using the 5th edition of the American college of radiology breast imaging reporting and data system (ACR BI-RADS)[®] standard, without prior knowledge of pathological classifications. Discrepancies in their assessments were resolved through consensus discussion. Assessment criteria included morphological type of lesions (mass, non-mass enhancement), number of lesions (single, multiple^[15]), and lesion size. For mass lesions, DCE early phase shapes (regular and irregular), margins (clear, unclear/spiculated), internal enhancement characteristics (homogeneous, heterogeneous, and rim enhancement); for non-mass enhancement lesions, distribution characteristics (focal, linear, segmental, regional, multiple regions, and diffuse), and internal enhancement features (homogeneous, heterogeneous, clumped, and clustered ring enhancement). T2WI internal signal characteristics (hypointense, isointense, and hyperintense) were evaluated with reference to DWI and DCE images at the same level, lesions showing uniformly high signals on DWI and/or early uniform enhancement on DCE with homogeneous T2-weighted signals were classified as isointense; lesions with ring-like high signals on DWI and/or early non-uniform/ring-like enhancement on DCE with heterogeneous T2 signals were classified as hypointense or hyperintense.

Using the ISP MRI post-processing workstation, ADC values of lesions were measured in the region of interest on DWI images with multiple b values (0, 50, 100, 200, 500, 1000, and 2000), while avoiding normal tissue, necrosis, hemorrhage, or artifact areas, and the average of three measurements was taken as the lesion's ADC value. On DCE images, regions of obvious intense enhancement within the lesion were delineated to generate time-intensity curves, recording early enhancement rate and kinetic curve pattern/time signal curve (TIC) (Type I = persistent, Type II = plateau, and Type III = washout).

Histopathology

The expression of ER, PR, HER-2 status, and Ki-67 index in tumors was confirmed by operation or puncture pathology for all patients. For ER- and PR-positive tumors, nuclear staining in $\geq 1\%$ was defined as positive, while $< 1\%$ was considered negative. HER-2 negative and 1+ were judged as HER-2 negative; 3+ was directly designated as HER-2 positive; cases with 2+ staining underwent further fluorescence *in situ* hybridization detection, with gene amplification defined as HER-2 positive and non-amplification as negative. Under high magnification microscope, Ki-67 expression was categorized as high when the percentage of positive staining cells was $\geq 14\%$ relative to background levels, and low when

$< 14\%$. Breast cancer was subclassified into four subtypes according to the expert consensus criteria from the 2017 St. Gallen International Breast Cancer Conference^[5] [Table 1].

Statistical analysis

Statistical analysis was performed using Statistical Package for the Social Sciences 23.0 software. Normally distributed quantitative data were expressed as means \pm standard deviations, and intergroup comparisons among the four subtypes were made using analysis of variance. Categorical data were presented as frequencies and percentages, and comparisons between count data were conducted using the Chi-square test. A significance level of $P < 0.05$ indicated statistical significance.

RESULTS

Comparison of clinical and pathological features of different molecular subtypes of breast cancer

The 134 patients with primary breast cancer confirmed by pathology were all female, aged 29~79 (48.7 ± 10.42) years old, the clinicopathological features are summarized in Table 2. This study included 22 cases of Luminal A subtype (16.4%), 82 cases of Luminal B subtype (61.2%), 13 cases of HER-2 overexpression subtype (9.7%), and 17 cases of TNBC (12.7%). Significant statistical differences were found in age, average Ki-67 index, and histological type among the four molecular subtypes of breast cancer ($P = 0.025$; $P < 0.001$; $P < 0.001$). The HER-2(+) subtype demonstrated the highest median age at diagnosis (53.7 ± 12.8), while TNBC exhibited the youngest onset age (45.2 ± 7.8). TNBC exhibited the highest average Ki-67 index (60.0 ± 26.7). Among invasive ductal carcinoma cases, TNBC was the most prevalent subtype. In contrast, ductal carcinoma *in situ* (DCIS) was more commonly associated with the HER-2 (+) subtype. Notably, there were no statistically significant differences in menopausal status ($P = 0.380$) or axillary node metastasis across the molecular subtypes ($P = 0.446$).

Comparison of MRI morphological and signal features of different subtypes of breast cancer

Table 3 summarizes the MRI features of breast cancer molecular subtypes, with 93 cases showing masses (69.4%) and 41 cases showing non-mass enhancement (30.6%). No statistically significant association was observed between molecular subtypes and lesion morphological types ($P = 0.061$); however, non-mass enhancement patterns with HER-2 (+) [Figure 1] were the most common, accounting for 61.5% of cases.

Statistical analysis revealed significant variations in morphological characteristics of mass lesions across

molecular subtypes, including shape ($P = 0.039$), margin ($P < 0.001$), internal enhancement pattern ($P = 0.043$), and T2WI signal intensity ($P = 0.014$). Luminal A [Figure 2] and lumina B [Figure 3] subtypes typically demonstrated irregular shapes, unclear or spiculated margins, heterogeneous enhancement on DCE, and predominantly heterogeneous low or iso-signal on T2WI, while TNBC [Figure 4] frequently appeared as round or regular shapes (71.4%) with clear margins, predominantly ring enhancement on DCE (50%), and heterogeneous high signal on T2WI (52.9%). T2 signal homogeneity analysis showed significant disparities: Luminal A subtype (68.2%) and HER-2 (+) subtypes (69.2%) exhibited higher rates of homogeneous isointense signals compared to Luminal B (46.3%) and TNBC (35.3%) ($P = 0.014$). Non-mass enhancement features predominantly displayed lobular segmental distribution with clumped or clustered ring enhancement patterns, though these differences did not reach statistical significance across subtypes ($P = 0.080$; $P = 0.301$,

respectively). Multifocal/multicentric or bilateral disease occurred in 23.1% of cases, with Luminal B representing the most frequent subtype (29.3%, $P = 0.181$). While no significant correlation emerged between tumor size and molecular subtypes ($P = 0.137$), dimensional analysis revealed that HER-2 (+) tumors had the largest mean diameter (3.8 ± 1.8 cm) compared to Luminal A (2.3 ± 1.7 cm).

Comparison ADC value of breast cancer in different molecular subtypes

Quantitative ADC analysis revealed statistically significant differences in mean ADC values across molecular subtypes ($P < 0.001$) [Figure 5]. The mean ADC values of HER-2 overexpressed breast cancer ($0.98 \pm 0.23 \times 10^{-3}$ mm²/s) were higher than those of the other three subtypes, and those of luminal types were lower than non-luminal groups.

Comparison DCE hemodynamics of breast cancer in different molecular subtypes

There were statistical differences in the DCE early enhancement rate and kinetic curve patterns of breast cancer lesions with different molecular subtypes ($P = 0.009$; $P = 0.020$, respectively) [Figure 5]. Quantitative analysis revealed Luminal A tumors demonstrated the highest mean early-phase enhancement rate ($206.7\% \pm 75.6$), contrasting with HER-2 (+) subtypes which showed the lowest enhancement ($157.5\% \pm 48.0$). While all four subtypes predominantly exhibited type III washout kinetics, substantial variations

Table 1: Breast cancer molecular subtypes.

Molecular Subtype	ER and PR	HER-2	Ki-67
Luminal A	ER+and/or PR+	HER-2-	<14%
Luminal B	ER+and/or PR±	HER-2-	≥14%
	ER+and/or PR±	HER-2+	Any
HER-2 (+)	ER-, PR-	HER-2+	Any
TNBC	ER-, PR-	HER-2-	Any

ER: Estrogen receptor, PR: Progesterone receptor, HER-2: Human epidermal growth factor receptor-2, TNBC: Triple-negative breast cancer

Table 2: Clinicopathological features stratified by molecular subtypes.

Clinicopathological feature	Luminal A (n=22)	Luminal B (n=82)	HER-2 (+) (n=13)	TNBC (n=17)	P-value
Age, years	52.8±11.0	47.6±9.9	53.7±12.8	45.2±7.8	0.025
Ki-67 index	9.0±2.3	39.9±18.7	39.6±23.5	60.0±26.7	<0.001
Pathological type (%)					
IDC	17 (77.3)	68 (82.9)	5 (38.5)	17 (100)	<0.001
DCIS	1 (4.5)	2 (2.4)	7 (53.8)	0 (0)	
ILC	2 (9.1)	4 (4.9)	0 (0)	0 (0)	
Mucinous carcinoma	0 (0)	4 (4.9)	0 (0)	0 (0)	
IMPC	0 (0)	4 (4.9)	0 (0)	0 (0)	
Medullary carcinoma	0 (0)	0 (0)	1 (7.7)	0 (0)	
IPC	2 (9.1)	0 (0)	0 (0)	0 (0)	
Menopausal state					
Premenopausal	13 (59.1)	52 (63.4)	5 (38.5)	11 (64.7)	0.380
Postmenopausal	9 (40.9)	31 (36.6)	8 (61.5)	6 (35.3)	
Lymph Node Status					
Negative	16 (72.7)	44 (53.7)	8 (61.5)	10 (58.8)	0.446
Positive	6 (27.3)	38 (46.3)	5 (38.5)	7 (41.2)	

IDC: Invasive ductal carcinoma, DCIS: Ductal carcinoma *in situ*, ILC: Invasive lobular carcinoma, IMPC: Invasive micropapillary carcinoma, IPC: Intraductal papillary carcinoma, HER-2: Human epidermal growth factor receptor-2, TNBC: Triple-negative breast cancer

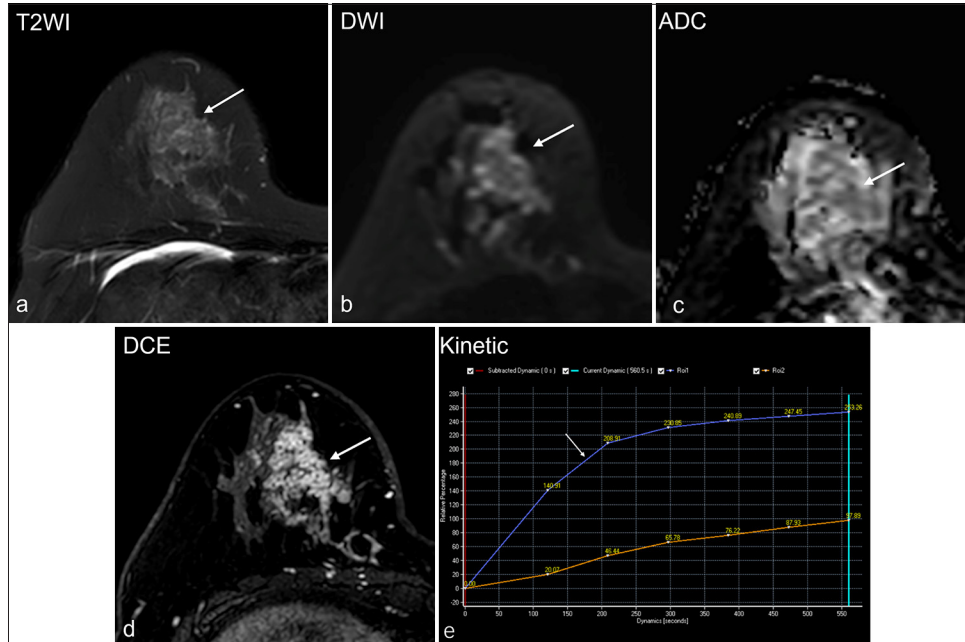


Figure 1: A 40-year-old woman diagnosed with invasive ductal carcinoma of the human epidermal growth factor receptor-2 subtype. (a) The lesion presents isointense on T2-weighted imaging (white arrow), (b) uneven high signal on diffusion-weighted imaging (white arrow), (c) corresponding low signal on apparent diffusion coefficient (ADC) mapping (white arrow), the average ADC value is $1.31 \times 10^{-3} \text{mm}^2/\text{s}$. (d) The initial phase of dynamic contrast enhancement shows a segmental clustered ring enhancement (white arrow), (e) the kinetic curve (white arrow) demonstrates a persistent appearance (type I curve). (T2WI: T2-weighted imaging, DWI: Diffusion-weighted imaging, DCE: Dynamic contrast enhancement)

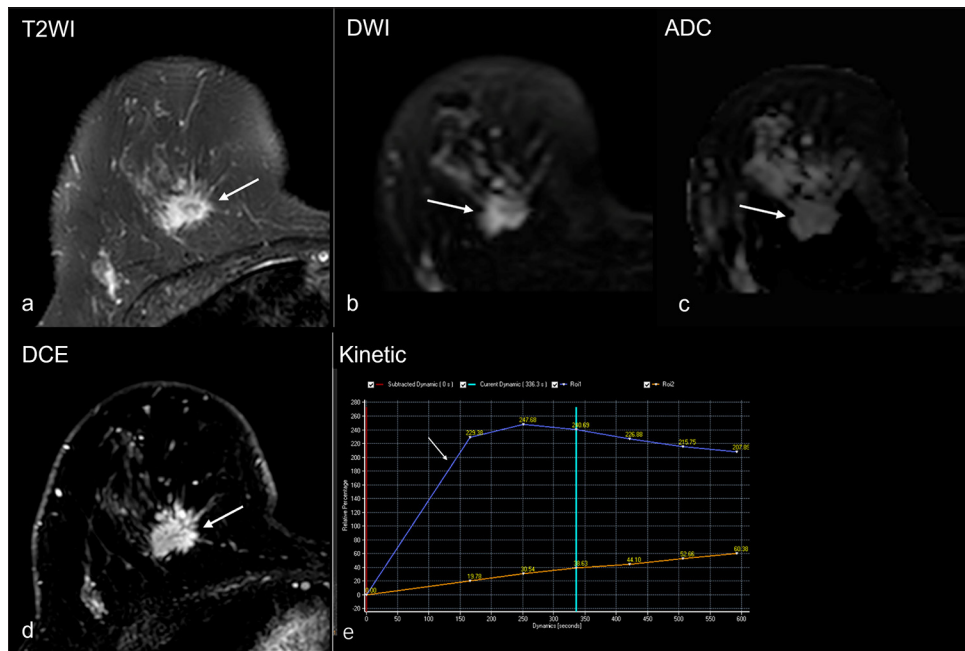


Figure 2: A 45-year-old woman diagnosed with invasive ductal carcinoma of the Luminal A subtype. (a) The lesion presents uneven low signal on T2-weighted imaging (white arrow), (b) uneven high signal on diffusion-weighted imaging (white arrow), (c) corresponding low signal on apparent diffusion coefficient (ADC) mapping (white arrow), the average ADC value is $0.71 \times 10^{-3} \text{mm}^2/\text{s}$. (d) The initial phase of dynamic contrast enhancement shows a heterogeneous internal enhanced mass with irregular shape and spiculated margin (white arrow), (e) the kinetic curve (white arrow) demonstrates a plateau appearance (type II curve). (T2WI: T2-weighted imaging, DWI: Diffusion-weighted imaging, DCE: Ddynamic contrast enhancement)

Table 3: MRI imaging features of 134 cases with different molecular subtype.					
MRI imaging feature	Luminal A (n=22)	Luminal B (n=82)	HER-2 (+) (n=13)	TNBC (n=17)	P-value
Tumor location (%)					
Right	12 (54.5)	46 (56.1)	8 (61.5)	11 (64.7)	0.711
Left	10 (45.5)	35 (42.7)	5 (38.5)	5 (29.4)	
Bilateral	0 (0)	1 (1.2)	0 (0)	1 (5.9)	
Lesion Type (%)					
Mass	16 (72.7)	58 (70.7)	5 (38.5)	14 (82.4)	0.061
NME	6 (27.3)	24 (29.3)	8 (61.5)	3 (17.6)	
Tumor number (%)					
Unifocal	19 (86.4)	58 (70.7)	12 (92.3)	14 (82.4)	0.181
Multifocal	3 (13.6)	24 (29.3)	1 (7.7)	3 (17.6)	
Size	2.3±1.7	2.9±1.9	3.8±1.8	2.6±1.6	0.137
T2 intensity (%)					
Hypointense	6 (27.3)	24 (29.3)	1 (7.7)	2 (11.8)	0.014
Isointense	15 (68.2)	38 (46.3)	9 (69.2)	6 (35.3)	
Hyperintense	1 (4.5)	20 (24.4)	3 (23.1)	9 (52.9)	
ADC value	0.72±0.18	0.70±0.13	0.98±0.23	0.78±0.19	<0.001
Early strengthening rate	206.7±75.6	165.6±51.5	157.5±48.0	188.5±45.8	0.009
Kinetic curve pattern (%)					
I	0 (0)	7 (8.5)	3 (23.1)	0 (0)	0.020
II	2 (9.1)	22 (26.8)	5 (38.5)	3 (17.6)	
III	20 (90.9)	53 (64.6)	5 (38.5)	14 (82.4)	
Mass	(n=16)	(n=58)	(n=5)	(n=14)	
Shape (%)					
Regular	5 (31.3)	19 (32.8)	1 (20)	10 (71.4)	0.039
Irregular	11 (68.7)	39 (67.2)	4 (80)	4 (28.6)	
Margin (%)					
Circumscribed	3 (18.8)	15 (25.9)	1 (20)	12 (85.7)	<0.001
Uneven/spiculated	13 (81.2)	43 (74.1)	4 (80)	2 (14.3)	
Enhancement characteristic (%)					
Homogeneous	4 (25)	6 (10.3)	2 (40)	1 (7.1)	0.043
Heterogeneous	9 (56.3)	41 (70.7)	1 (20)	6 (42.9)	
Rim	3 (18.8)	11 (19.0)	2 (40)	7 (50)	
NME	(n=6)	(n=24)	(n=8)	(n=3)	
Distribution (%)					
Focal	0 (0)	4 (16.7)	0 (0)	2 (66.7)	0.080
Linear	2 (33.3)	1 (4.2)	0 (0)	0 (0)	
Segmental	2 (33.3)	13 (54.2)	7 (87.5)	0 (0)	
Regional	2 (33.3)	3 (12.5)	0 (0)	1 (33.3)	
M regions	0 (0)	2 (8.3)	1 (12.5)	0 (0)	
Diffuse	0 (0)	1 (4.2)	0 (0)	0 (0)	
Enhancement Patterns (%)					
Homogeneous	1 (16.7)	1 (4.2)	1 (12.5)	0 (0)	0.301
Heterogenous	1 (16.7)	3 (12.5)	0 (0)	2 (66.7)	
Clumped	2 (33.3)	12 (50)	3 (37.5)	0 (0)	
Cluster ring	2 (33.3)	8 (33.3)	4 (50)	1 (33.3)	

MRI: Magnetic resonance imaging, ADC: Apparent diffusion coefficient, NME: Non-mass enhancement, HER-2: Human epidermal growth factor receptor-2, TNBC: Triple-negative breast cancer

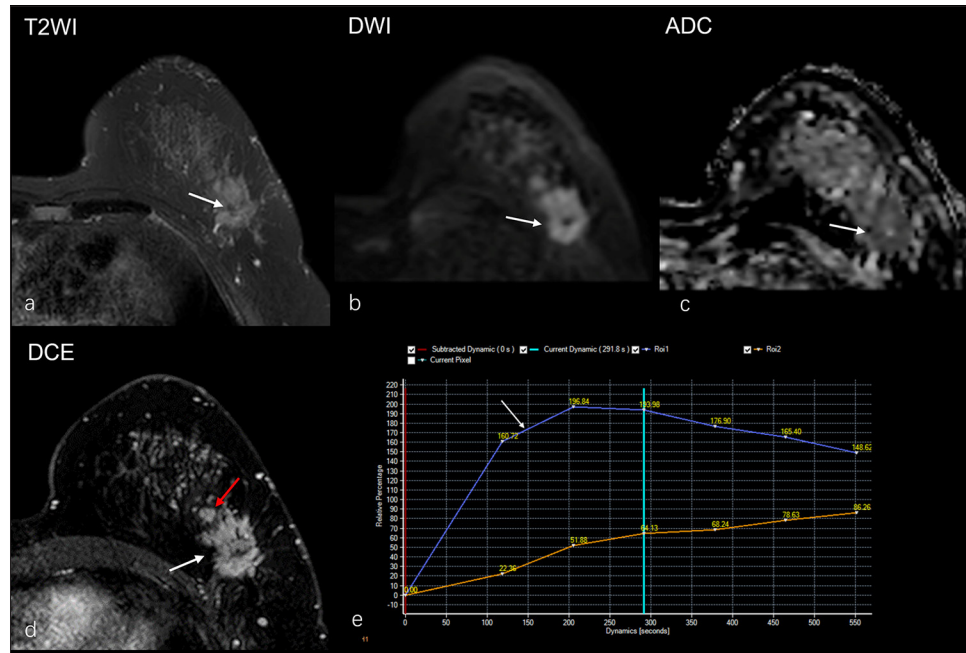


Figure 3: A 52-year-old woman diagnosed with invasive ductal carcinoma of the Luminal B subtype. (a) The lesion presents uneven low signal on T2-weighted imaging (white arrow), (b) uneven high signal on diffusion-weighted imaging (white arrow), (c) corresponding low signal on apparent diffusion coefficient (ADC) mapping (white arrow), the average ADC value is $0.72 \times 10^{-3} \text{mm}^2/\text{s}$. (d) The initial phase of dynamic contrast enhancement shows a heterogeneous internal enhanced mass with irregular shape and spiculated margin (white arrow), and a daughter lesion in front of the mass (red arrow), (e) the kinetic curve (white arrow) demonstrates a wash out appearance (type III curve). (T2WI: T2-weighted imaging, DWI: Diffusion-weighted imaging, DCE: Dynamic contrast enhancement)

emerged in distribution patterns: 90.9% of Luminal A and 82.4% of TNBC displayed type III curves, compared to 64.6% in Luminal B and only 38.5% in HER-2 (+) subtypes. Notably, HER-2 (+) tumors predominantly demonstrated type I (persistent) or II (plateau) kinetic patterns (61.6% combined prevalence).

DISCUSSION

Breast cancer exhibits diverse MRI features, with mass and non-mass enhancement being the two primary presentations. Our findings confirm that mass enhancement is more commonly observed, which is consistent with previous research.^[7,9,16-19] Notably, our study revealed that HER-2 overexpression was most frequently associated with non-mass enhancement, while TNBC predominated in mass type.

The MRI features identified in our study can be linked to underlying biological mechanisms and carry significant clinical implications. For instance, HER-2-overexpressing breast cancers typically exhibit a non-mass, comedo-like morphology with intraductal growth, which contains a higher proportion of DCIS compared to other subtypes. Moreover, the non-mass enhancement observed in HER-2-overexpressing tumors, often characterized by

segmental or clustered ring enhancement, may reflect the tumor's microinvasive growth pattern and ductal spread. This pattern is often associated with necrotic calcifications, which can be identified on mammography.^[7,10,18,20-22] These insights may inform targeted biopsy strategies by guiding attention to regions exhibiting these specific MRI features, ultimately enhancing diagnostic accuracy and personalizing patient management.

Similarly, the regular shape and well-defined margins of TNBC lesions observed on MRI may indicate a rapid growth pattern characterized by expansive pushing rather than infiltrative behavior. This distinctive feature could aid in differentiating TNBC from other subtypes, potentially influencing treatment decisions and prognostic assessments. Kazama *et al.*^[23] reported that TNBC types are more frequently presented as masses, tend to be solitary, and have a larger diameter. Researchers such as Megumi have proposed a negative correlation between tumor roundness and ER expression, while observing a positive correlation with the Ki-67 index.^[24] These findings align closely with the results obtained in our study.

Domestic and international studies have consistently shown that irregular shapes and irregular or spiculated

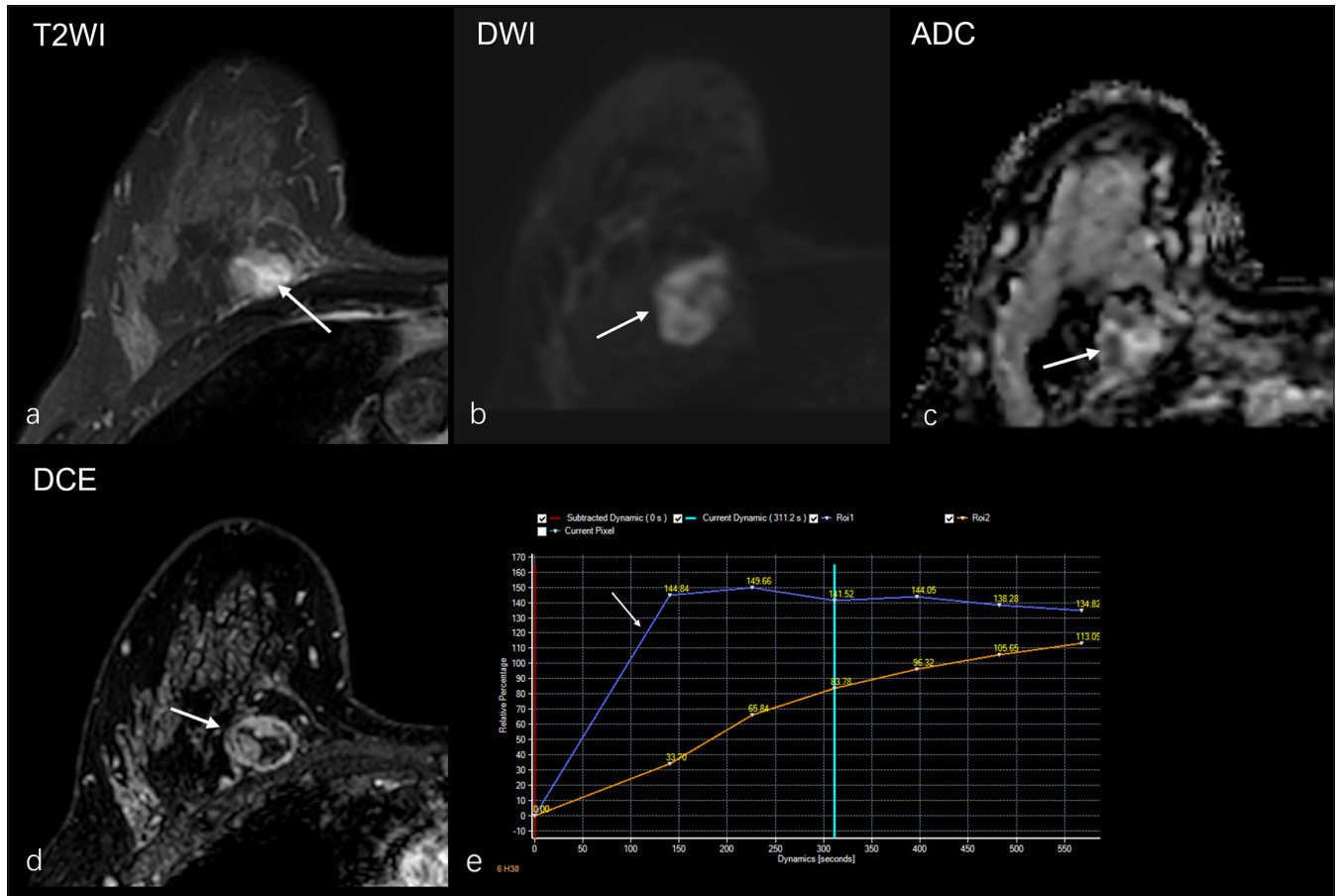


Figure 4: A 35-year-old woman diagnosed with invasive ductal carcinoma of the triple-negative breast cancer. (a) The lesion presents uneven high signal on T2-weighted imaging (white arrow), (b) circular high signal on diffusion-weighted imaging (white arrow), (c) corresponding circular low signal on apparent diffusion coefficient (ADC) mapping (white arrow), the average ADC value of the solid part is $0.84 \times 10^{-3} \text{mm}^2/\text{s}$. (d) The initial phase of dynamic contrast enhancement shows a round regular ring enhanced mass with smooth margin (white arrow), (e) the kinetic curve (white arrow) demonstrates a plateau appearance (type II curve). (T2WI: T2-weighted imaging, DWI: Diffusion-weighted imaging, DCE: Dynamic contrast enhancement)

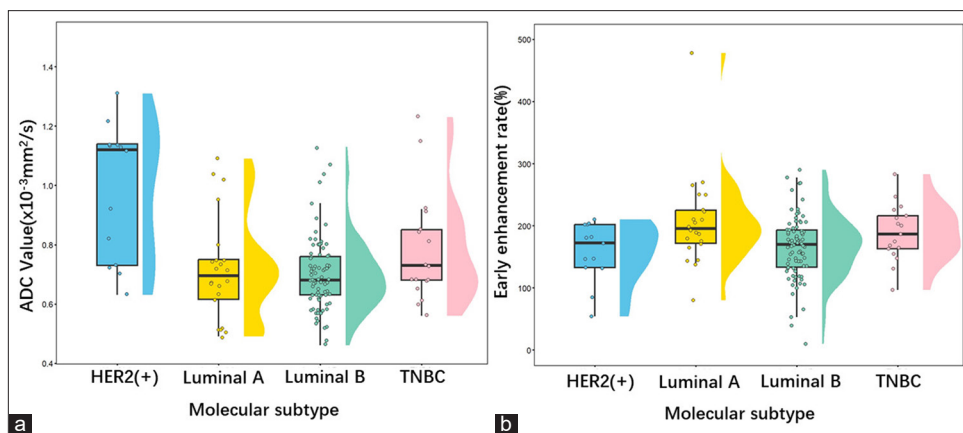


Figure 5: (a and b) Box plots show the differences of apparent diffusion coefficient (ADC) value and dynamic contrast enhancement early enhancement rate for the four molecular subtypes ($P < 0.001$; $P = 0.009$). The mean ADC values of human epidermal growth receptor-2 (HER-2) overexpressed breast cancer ($0.98 \pm 0.23 \times 10^{-3} \text{mm}^2/\text{s}$) were higher than those of the other three subtypes, and those of Luminal types were lower than non-Luminal groups. Quantitative analysis revealed Luminal A tumors demonstrated the highest mean early-phase enhancement rate ($206.7\% \pm 75.6$), contrasting with HER-2(+) subtypes which showed the lowest enhancement ($157.5\% \pm 48.0$).

margins are more common in luminal types with better prognosis.^[3,9,16,25-28] Our study similarly corroborates these findings. The MRI imaging characteristics of luminal tumors are linked to slower tumor growth and earlier disease staging, suggesting a less aggressive and invasive biological behavior. This may be attributed to connective tissue hyperplasia, which acts as a physical barrier limiting tumor expansion.^[9,29] Furthermore, research by Lamb *et al.*^[30] has demonstrated a correlation between spiculated signs and the expression of *ER/PR* genes, underscoring the significant prognostic value of MRI features in predicting tumor behavior and clinical outcomes.

TNBC showed ring enhancement in DCE and uneven hyperintense on T2WI, in contrast, luminal subtypes predominantly demonstrated heterogeneous enhancement with predominantly hypointense or isointense signals on T2WI, findings that are consistent with prior research.^[3,10,29,31,32] The magnetic resonance features of TNBC are associated with its “basal-like” composition,^[10] characterized by high marginal microvascular density at the tumor periphery. This leads to hypoxia and necrosis during rapid tumor growth,^[33] which manifests as ring enhancement patterns and heterogeneous high signals on T2WI due to necrotic and cystic changes within the tumor. On the other hand, luminal lesions displayed heterogeneous enhancement with relatively low-signal intensity on T2WI, corresponding to fibrous scar formation within the tumor. This reflects hypoxia-driven stromal formation, compared to tumors with homogeneous signal characteristics, the presence of fibrotic foci in the lesion center may indicate a worse prognosis, suggesting that these imaging features could serve as potential biomarkers for assessing tumor behavior and clinical outcomes.^[10]

The correlation between molecular subtypes of breast cancer and TIC remains a controversial in both domestic and international research. Some scholars argue that there is no significant association between TIC curves and molecular subtypes.^[7,26,29] However, our study reveals statistically significant differences in the early enhancement rate and TIC types among different subtypes. Luminal A subtype exhibited the highest average early enhancement rate, while HER-2 (+) type demonstrated the lowest. The washout pattern observed in Luminal A and TNBC may result from shorter mean transit times and higher outflow rates, indicating faster contrast agent clearance due to more permeable vasculature or enhanced lymphatic drainage.^[24] In contrast, the HER-2 (+) subtype predominantly exhibits non-mass enhancement, influenced by the surrounding normal breast tissue, leading to Type I or Type II TIC curves. This suggests slower contrast uptake and retention, reflecting the unique vascular architecture and microenvironment of HER-2-overexpressing tumors. These MRI-based insights into TIC patterns and molecular subtypes hold significant potential

for guiding clinical decision-making. For instance, the distinct TIC profiles of different subtypes can inform targeted biopsy strategies, allowing clinicians to focus on regions with specific enhancement patterns that correlate with aggressive tumor behavior.

Our study confirmed that breast cancers with HER-2 overexpression had higher mean ADC values compared to the other three subtypes, consistent with prior findings.^[11,12,26,34] This may result from *HER-2* gene amplification and high expression, which drive active cell proliferation and increased tumor angiogenesis. However, the incomplete vascular walls in these tumors lead to high permeability and enhanced water molecule diffusion. In addition, HER-2 overexpression often presents as non-mass enhancement, influenced by surrounding normal breast tissue, further contributing to higher ADC values. In contrast, our results showed lower ADC values in luminal types compared to HER-2(+) and TNBC, aligning with Moradi *et al.*^[26] This difference likely reflects distinct biological behaviors, such as the fibrous stromal components and slower water diffusion seen in luminal tumors due to their less aggressive growth patterns. These MRI insights into ADC values have important clinical implications. Higher ADC values in HER-2 overexpression suggest less invasive behavior, potentially guiding less extensive surgery or targeted therapies. Lower ADC values in luminal types indicate denser tumor structures, influencing biopsy strategies by highlighting areas with restricted diffusion that may harbor more aggressive regions. Furthermore, understanding these differences can aid in treatment planning, such as selecting appropriate neoadjuvant chemotherapy or predicting endocrine therapy responses in luminal subtypes.

Literature has shown that multifocality/multicentricity correlates with Luminal B and HER-2(+) subtypes.^[3,7,35] While our study did not find statistical difference, multifocal/multicentric breast cancer was mostly associated with Luminal B subtype.

This study has several limitations that warrant consideration. First, the retrospective design introduces potential biases, including inter-reader variability in MRI interpretation. The reliance on subjective radiologist assessments of MRI characteristics may compromise diagnostic reproducibility, potentially impacting the reliability of our observations. Second, the modest cohort size coupled with disproportionate representation across molecular subtypes raises concerns regarding statistical robustness and broader clinical generalizability. We propose that subsequent research employ prospective multicenter studies with expanded sample sizes, thereby enhancing statistical power through balanced subgroup stratification. Of particular note, the current findings lack external validation through independent cohorts, which restrict comprehensive evaluation of both

technical reproducibility and translational potential. Our research group intends to pursue collaborative validation initiatives across multiple institutions to strengthen the clinical relevance of these preliminary results.

CONCLUSION

Multiparametric MRI features, particularly ADC values, DCE kinetics, and T2WI signals, demonstrate significant associations with breast cancer molecular subtypes. These imaging biomarkers offer potential for non-invasive subtype prediction, supporting more tailored diagnostic and treatment strategies.

Ethical approval: The research/study was approved by the Institutional Review Board at Xiangyang No.1 People's Hospital, number XYYYE20220091, dated September 08, 2022.

Declaration of patient consent: The authors certify that they have obtained all appropriate patient consent.

Financial support and sponsorship: The study was supported by Hubei Provincial Natural Science Foundation (Grants number: 2025AFD093), Faculty Development Grants of Xiangyang No.1 People's Hospital Affiliated to Hubei University of Medicine (Grants number: XYY2023D02) and Innovative Research Program of Xiangyang No. 1 People's Hospital (Grants number: XYY2023QT01).

Conflicts of interest: There are no conflicts of interest.

Use of artificial intelligence (AI)-assisted technology for manuscript preparation: The authors confirm that there was no use of artificial intelligence (AI)-assisted technology for assisting in the writing or editing of the manuscript and no images were manipulated using AI.

REFERENCES

1. Siegel RL, Miller KD, Fuchs HE, Jemal A. Cancer statistics, 2021. *CA Cancer J Clin* 2021;71:7-33.
2. Zhang Y, Chen JH, Lin Y, Chan S, Zhou J, Chow D, *et al.* Prediction of breast cancer molecular subtypes on DCE-MRI using convolutional neural network with transfer learning between two centers. *Eur Radiol* 2021;31:2559-67.
3. Chen H, Li W, Wan C, Zhang J. Correlation of dynamic contrast-enhanced MRI and diffusion-weighted MR imaging with prognostic factors and subtypes of breast cancers. *Front Oncol* 2022;12:942943.
4. Prat A, Pineda E, Adamo B, Galván P, Fernández A, Gaba L, *et al.* Clinical implications of the intrinsic molecular subtypes of breast cancer. *Breast* 2015;24 Suppl 2:S26-35.
5. Goldhirsch A, Winer EP, Coates AS, Gelber RD, Piccart-Gebhart M, Thürlimann B, *et al.* Personalizing the treatment of women with early breast cancer: Highlights of the St Gallen International Expert Consensus on the Primary Therapy of Early Breast Cancer 2013. *Ann Oncol* 2013;24:2206-23.
6. Kondov B, Milenkovic Z, Kondov G, Petrushevska G, Basheska N, Bogdanovska-Todorovska M, *et al.* Presentation of the molecular subtypes of breast cancer detected by immunohistochemistry in surgically treated patients. *Open Access Maced J Med Sci* 2018;6:961-7.
7. Seyfettin A, Dede I, Hakverdi S, Düzel Asig B, Temiz M, Karazincir S. MR imaging properties of breast cancer molecular subtypes. *Eur Rev Med Pharmacol Sci* 2022;26:3840-8.
8. Almendro V, Fuster G. Heterogeneity of breast cancer: Etiology and clinical relevance. *Clin Transl Oncol* 2011;13:767-73.
9. Szep M, Pintican R, Boca B, Perja A, Duma M, Feier D, *et al.* Multiparametric MRI Features of breast cancer molecular subtypes. *Medicina (Kaunas)* 2022;58:1716.
10. Yuen S, Monzawa S, Yanai S, Matsumoto H, Yata Y, Ichinose Y, *et al.* The association between MRI findings and breast cancer subtypes: Focused on the combination patterns on diffusion-weighted and T2-weighted images. *Breast Cancer* 2020;27:1029-37.
11. Kim JJ, Kim JY, Suh HB, Hwangbo L, Lee NK, Kim S, *et al.* Characterization of breast cancer subtypes based on quantitative assessment of intratumoral heterogeneity using dynamic contrast-enhanced and diffusion-weighted magnetic resonance imaging. *Eur Radiol* 2022;32:822-33.
12. Kang HS, Kim JY, Kim JJ, Kim S, Lee NK, Lee JW, *et al.* Diffusion Kurtosis MR imaging of invasive breast cancer: Correlations with prognostic factors and molecular subtypes. *J Magn Reson Imaging* 2022;56:110-20.
13. Kettunen T, Okuma H, Auvinen P, Sudah M, Tiainen S, Sutela A, *et al.* Peritumoral ADC values in breast cancer: Region of interest selection, associations with hyaluronan intensity, and prognostic significance. *Eur Radiol* 2020;30:38-46.
14. Cho N. Imaging features of breast cancer molecular subtypes: State of the art. *J Pathol Transl Med* 2021;55:16-25.
15. Milulescu A, Di Marino L, Peradze N, Toesca A. Management of multifocal-multicentric breast cancer: Current perspective. *Chirurgia (Bucur)* 2017;112:12-7.
16. Adrada BE, Moseley TW, Kapoor MM, Scoggins ME, Patel MM, Perez F, *et al.* Triple-negative breast cancer: Histopathologic features, genomics, and treatment. *Radiographics* 2023;43:e230034.
17. Grimm LJ, Zhang J, Baker JA, Soo MS, Johnson KS, Mazurowski MA. Relationships between MRI breast imaging-reporting and data system (BI-RADS) lexicon descriptors and breast cancer molecular subtypes: Internal enhancement is associated with luminal B subtype. *Breast J* 2017;23:579-82.
18. Asada T, Yamada T, Kanemaki Y, Fujiwara K, Okamoto S, Nakajima Y. Grading system to categorize breast MRI using BI-RADS 5th edition: A statistical study of non-mass enhancement descriptors in terms of probability of malignancy. *Jpn J Radiol* 2018;36:200-8.
19. Costantini M, Belli P, Distefano D, Bufi E, Matteo MD, Rinaldi P, *et al.* Magnetic resonance imaging features in triple-negative breast cancer: Comparison with luminal and HER2-overexpressing tumors. *Clin Breast Cancer* 2012;12:331-9.
20. McAndrew NP. Updates on targeting human epidermal growth factor receptor 2-positive breast cancer: What's to know in 2021. *Curr Opin Obstet Gynecol* 2022;34:41-5.
21. Van den Eynden GG, Colpaert CG, Couvelard A, Pezzella F, Dirix LY, Vermeulen PB, *et al.* A fibrotic focus is a prognostic factor and a surrogate marker for hypoxia and (lymph) angiogenesis in breast cancer: Review of the literature and proposal on the criteria of evaluation. *Histopathology*

- 2007;51:440-51.
22. Aydin H. The MRI characteristics of non-mass enhancement lesions of the breast: Associations with malignancy. *Br J Radiol* 2019;92:20180464.
 23. Kazama T, Takahara T, Hashimoto J. Breast cancer subtypes and quantitative magnetic resonance imaging: A systemic review. *Life (Basel)* 2022;12:490.
 24. Matsumoto M, Yamaguchi R, Morita M, Mizushima Y, Amamoto T. Relationships between histomorphology, imaging findings and subtypes in breast cancer. *Nihon Hoshasen Gijutsu Gakkai Zasshi* 2022;78:1224-9.
 25. Song SE, Bae MS, Chang JM, Cho N, Ryu HS, Moon WK. MR and mammographic imaging features of HER2-positive breast cancers according to hormone receptor status: A retrospective comparative study. *Acta Radiol* 2017;58:792-9.
 26. Moradi B, Gity M, Etesam F, Borhani A, Ahmadijead N, Kazemi MA. Correlation of apparent diffusion coefficient values and peritumoral edema with pathologic biomarkers in patients with breast cancer. *Clin Imaging* 2020;68:242-8.
 27. Öztürk VS, Polat YD, Soyder A, Tanyeri A, Karaman CZ, Taşkın F. The Relationship between MRI findings and molecular subtypes in women with breast cancer. *Curr Probl Diagn Radiol* 2020;49:417-21.
 28. Angelini G, Marini C, Iacconi C, Mazzotta D, Moretti M, Picano E, *et al.* Magnetic resonance (MR) features in triple negative breast cancer (TNBC) vs receptor positive cancer (nTNBC). *Clin Imaging* 2018;49:12-6.
 29. Navarro Vilar L, Alandete Germán SP, Medina García R, Blanc García E, Camarasa Lillo N, Vilar Samper J. MR imaging findings in molecular subtypes of breast cancer according to BIRADS system. *Breast J* 2017;23:421-8.
 30. Lamb PM, Perry NM, Vinnicombe SJ, Wells CA. Correlation between ultrasound characteristics, mammographic findings and histological grade in patients with invasive ductal carcinoma of the breast. *Clin Radiol* 2000;55:40-4.
 31. Youk JH, Son EJ, Chung J, Kim JA, Kim EK. Triple-negative invasive breast cancer on dynamic contrast-enhanced and diffusion-weighted MR imaging: Comparison with other breast cancer subtypes. *Eur Radiol* 2012;22:1724-34.
 32. Mujtaba SS, Ni YB, Tsang JY, Chan SK, Yamaguchi R, Tanaka M, *et al.* Fibrotic focus in breast carcinomas: Relationship with prognostic parameters and biomarkers. *Ann Surg Oncol* 2013;20:2842-9.
 33. Golshan M, Wong SM, Loibl S, Huober JB, O'Shaughnessy J, Rugo HS, *et al.* Early assessment with magnetic resonance imaging for prediction of pathologic response to neoadjuvant chemotherapy in triple-negative breast cancer: Results from the phase III BrighTNess trial. *Eur J Surg Oncol* 2020;46:223-8.
 34. Xie T, Zhao Q, Fu C, Bai Q, Zhou X, Li L, *et al.* Differentiation of triple-negative breast cancer from other subtypes through whole-tumor histogram analysis on multiparametric MR imaging. *Eur Radiol* 2019;29:2535-44.
 35. Ha R, Jin B, Mango V, Friedlander L, Miloshev V, Malak S, *et al.* Breast cancer molecular subtype as a predictor of the utility of preoperative MRI. *AJR Am J Roentgenol* 2015;204:1354-60.

How to cite this article: Li J, Huo G, Lei X, Li G, Yu M, Nie Z, *et al.* Correlation analysis of multiparametric magnetic resonance imaging features and molecular subtypes of breast cancer. *J Clin Imaging Sci.* 2025;15:37. doi: 10.25259/JCIS_162_2024